PUBLISHED ONLINE: 29 FEBRUARY 2012 | DOI: 10.1038/NPHOTON.2012.22
nature photonics

# The renaissance of dye-sensitized solar cells

Brian E. Hardin[1], Henry J. Snaith[2] and Michael D. McGehee[3*]

**Several recent major advances in the design of dyes and electrolytes for dye-sensitized solar cells have led to record power-conversion efficiencies. Donor–pi–acceptor dyes absorb much more strongly than commonly employed ruthenium-based dyes, thereby allowing most of the visible spectrum to be absorbed in thinner films. Light-trapping strategies are also improving photon absorption in thin films. New cobalt-based redox couples are making it possible to obtain higher open-circuit voltages, leading to a new record power-conversion efficiency of 12.3%. Solid-state hole conductor materials also have the potential to increase open-circuit voltages and are making dye-sensitized solar cells more manufacturable. Engineering the interface between the titania and the hole transport material is being used to reduce recombination and thus attain higher photocurrents and open-circuit voltages. The combination of these strategies promises to provide much more efficient and stable solar cells, paving the way for large-scale commercialization.**

Dye-sensitized solar cells (DSCs) are attractive because they are made from cheap materials that do not need to be highly purified and can be printed at low cost[1]. DSCs are unique compared with almost all other kinds of solar cells in that electron transport, light absorption and hole transport are each handled by different materials in the cell[2,3]. The sensitizing dye in a DSC is anchored to a wide-bandgap semiconductor such as $TiO_2$, $SnO_2$ or ZnO. When the dye absorbs light, the photoexcited electron rapidly transfers to the conduction band of the semiconductor, which carries the electron to one of the electrodes[4]. A redox couple, usually comprised of iodide/triiodide ($I^-/I_3^-$), then reduces the oxidized dye back to its neutral state and transports the positive charge to the platinized counter-electrode[5].

In 1991, O'Regan and Grätzel demonstrated that a film of titania ($TiO_2$) nanoparticles deposited on a DSC would act as a mesoporous n-type photoanode and thereby increase the available surface area for dye attachment by a factor of more than a thousand[1]. This approach dramatically improved light absorption and brought power-conversion efficiencies into a range that allowed the DSC to be viewed as a serious competitor to other solar cell technologies[6]. A schematic and energy level diagram showing the operation of a typical DSC is shown in Fig. 1. During the 1990s and the early 2000s, researchers found that organometallic complexes based on ruthenium provided the highest power-conversion efficiencies[7,8]. Iodide/triiodide was found to be the most effective redox couple[9–13]. The record power-conversion efficiency rapidly climbed to 10% in the late 1990s and then slowly settled to 11.5%[14–17]. Figure 2 shows a current–voltage curve under 1 Sun illumination, together with a plot of the external quantum efficiency as a function of photon wavelength.

The iodide/triiodide system has been particularly successful in DSCs because of the slow recombination kinetics between electrons in the titania with the oxidized dye and the triiodide in the electrolyte, which leads to long-lived electron lifetimes (between 1 ms and 1 s)[18–20]. Iodide reduces the oxidized dye to form an intermediate ionic species (such as $I_2^-$) that then disproportionates to form triiodide and diffuses to the counter-electrode, providing two electrons per molecule, as shown in Fig. 1b[4,19]. The slow recombination and relatively fast dye regeneration rates of the $I^-/I_3^-$ redox couple have resulted in near-unity internal quantum efficiencies for a large number of dyes, providing the high external quantum efficiencies shown in Fig. 2a. The small size of the $I^-/I_3^-$ redox components allows for relatively fast diffusion within the mesopores, and the two-electron system allows for a greater current to be passed for a given electrolyte concentration. Unfortunately, the $I^-/I_3^-$ system is corrosive and dissolves many of the commonly used sealants and metal interconnects (such as silver, copper, aluminium and gold).

## Obtaining maximum DSC power-conversion efficiencies

The Shockley–Queisser limit of ~32% is the maximum theoretical power-conversion efficiency of a single-junction solar cell device[21]. For highly efficient inorganic solar cells, the main deviation from this ideal limit is through the loss-in-potential, which can be roughly defined as the difference between the optical bandgap of the photoactive semiconductor divided by the charge of an electron, and the open-circuit voltage ($V_{OC}$). As an example, the record 25%-efficient silicon photovoltaic cell has a loss-in-potential of around 400 mV, whereas the record 28.1%-efficient GaAs device has a loss-in-potential of 300 mV (ref. 6). Unlike traditional inorganic solar cells, DSCs require relatively large over-potentials to drive electron injection to titania and regenerate the oxidized dye, as shown in Fig. 1b. This requirement results in significantly large loss-in-potentials of more than 700 mV and defines the minimum bandgap of the sensitizing dye (and therefore the onset of light absorption). A plot of the maximum obtainable efficiency versus loss-in-potential and absorption onset is shown in Fig. 3[22]. Typically, a potential difference between the lowest unoccupied molecular orbital (LUMO) level of the dye and the conduction band of titania is required for fast electron injection[3]. The magnitude of the required offset has not been precisely determined but is likely to be around 100–150 mV (ref. 23), which is much lower than the over-potential usually required to regenerate the dye. Regeneration of a ruthenium metal complex dye with the $I^-/I_3^-$ redox couple has a loss of around 600 mV, with over 300 mV of that being directly related to the reaction within the iodide electrolyte[4,19]. We estimate that the lowest loss-in-potential for the ruthenium complex/iodide system is 750 mV, which limits the maximum obtainable conversion efficiency to 13.8%, as shown in Fig. 3[22].

There are two main ways in which the efficiency of a DSC can be improved: extend the light-harvesting region into the near-infrared (NIR), and lowering the redox potential of the electrolyte to increase $V_{OC}$. Using a dye that absorbs further into the NIR, say to

[1]The Molecular Foundry, Lawrence Berkeley National Laboratory, Berkeley, California 94720, USA. [2]Department of Physics, Clarendon Laboratory, University of Oxford, Oxford OX1 3PU, UK. [3]Department of Material Science and Engineering, Stanford University, Stanford, California 94305-4045, USA. *e-mail: mmcgehee@stanford.edu

PUBLISHED ONLINE: 29 FEBRUARY 2012 | DOI: 10.1038/NPHOTON.2012.22

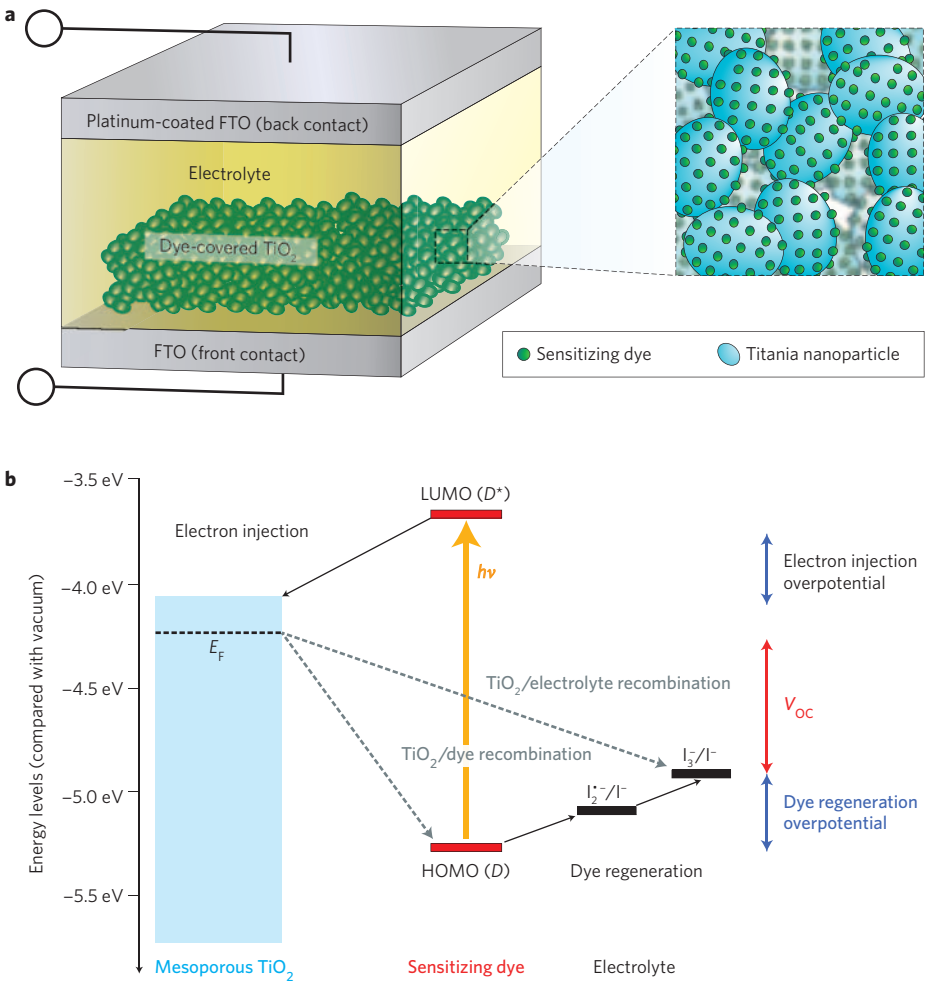


**Figure 1 | Dye-sensitized solar cell device schematic and operation. a**, Liquid-based DSCs are comprised of a transparent conducting oxide (such as fluorine-doped tin oxide, FTO) on glass, a nanoparticle photoanode (such as titania) covered in a monolayer of sensitizing dye, a hole-conducting electrolyte and a platinum-coated, FTO-coated glass back-contact[70]. **b**, Energy level and device operation of DSCs; the sensitizing dye absorbs a photon (energy $h\nu$), the electron is injected into the conduction band of the metal oxide (titania) and travels to the front electrode (not shown). The oxidized dye is reduced by the electrolyte, which is regenerated at the counter-electrode (not shown) to complete the circuit. $V_{OC}$ is determined by the Fermi level ($E_F$) of titania and the redox potential ($I_3^-/I^-$) of the electrolyte.

around 940 nm, while still managing to generate and collect the charge carriers efficiently, could increase the current by over 40%, as shown in Fig. 3[22,24]. Further increasing the power-conversion efficiency beyond 14% will require improved dyes and electrolytes with smaller over-potentials to efficiently transfer charge. Single-electron redox mediators based on cobalt and ferrocene complexes have two advantages over iodide. First, they do not require an intermediary step during regeneration and can therefore reduce the loss-in-potential. Second, unlike iodide, which does not have an ideal redox potential (0.35–0.40 eV over the normal hydrogen electrode), alternative electrolyte couples can be tuned closer to the highest occupied molecular orbital (HOMO) level of the sensitizing dye to obtain a higher $V_{OC}$.

Although efforts to solve these problems were stymied for many years[25], new approaches have recently emerged and the world-record efficiency is climbing again[26]. Over the past 15 years, there has been a great deal of research and improved understanding of the associated chemistry and device physics of DSCs, which is comprehensively described elsewhere[2–5,24,27–31]. This Review focuses on several recent promising innovations in the field that we believe will lead to power-conversion efficiencies of more than 15% in the near future.

## Strongly absorbing donor–pi–acceptor dyes

The sensitizing dye in a DSC is anchored to the n-type metal oxide surface[7]. Light absorption is determined by the molar extinction coefficient of the sensitizing dye, the surface coverage of the dye and the total surface area of the oxide film[29]. Sensitizing dyes generally pack tightly on the titania surface, with a density of 0.5–1 dye molecules per square nanometre[29]. Dyes typically contain a light-harvesting portion, acidic ligands (for example, carboxylic or phosphonic acid) to attach to the semiconductor surface, and ligands to increase the solubility in solution and reduce aggregation between dyes[7]. Aggregation occurs when the dye molecules are packed so tightly that their wavefunction overlap is large enough to change their electronic character, which often causes the dyes to quench in the excited state before electron transfer can occur.

Sensitizing dyes have traditionally been made from ruthenium-based complexes such as N3, N719, C106 and CYC B11[14,16,32], which have fairly broad absorption spectra ($\Delta\lambda \approx 350$ nm) but low molar extinction coefficients (10,000–20,000 $M^{-1}$ $cm^{-1}$)[15,33]. These complexes also have extremely weak absorption at the band-edge (around 780 nm), which restricts NIR light harvesting[22]. Although ruthenium-based complexes work well and have been the most widely used dyes over the past two decades, it seems that increased

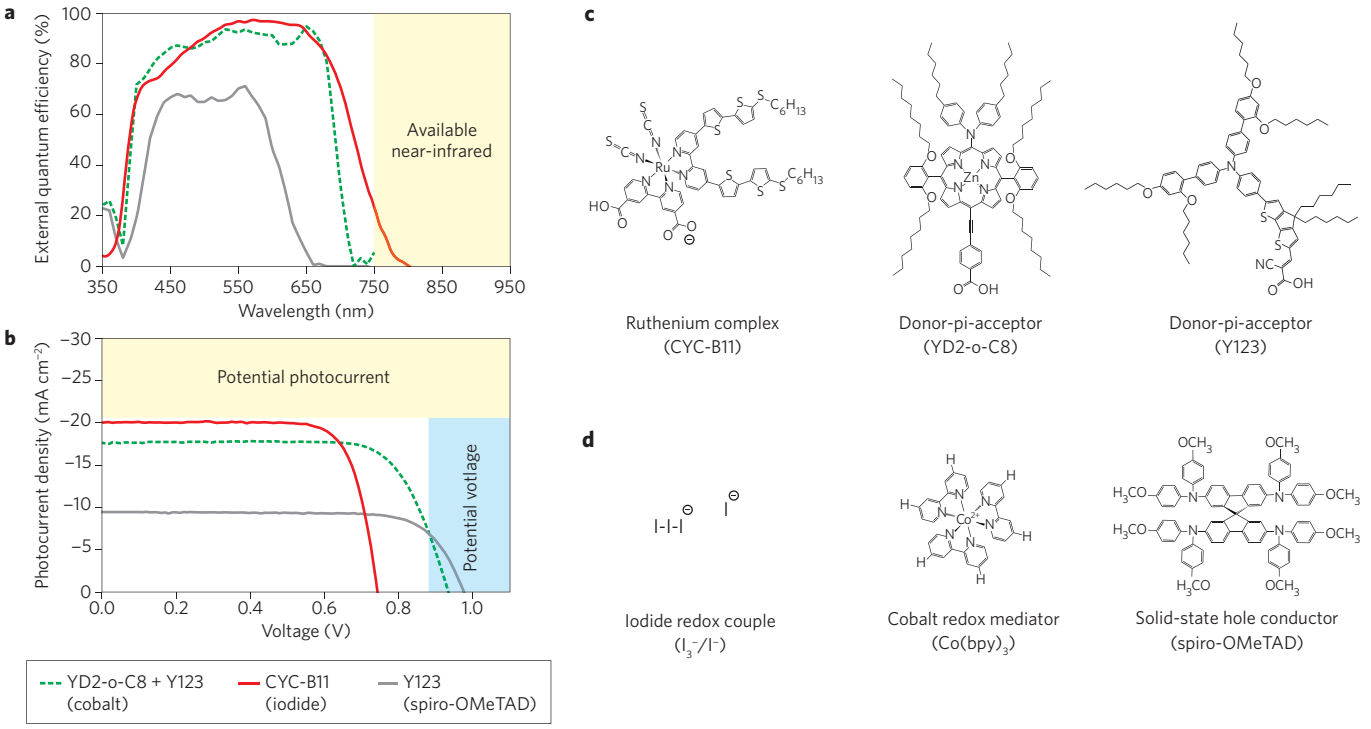


**Figure 2 | Best-in-class dye-sensitized solar cells. a**,**b**, The external quantum efficiency versus wavelength (**a**) and photocurrent density versus voltage (**b**) for the ruthenium dye (CYC-B11)/iodide redox couple[16], the co-sensitized donor–pi–acceptor dye (YD2-o-C8 and Y123)/cobalt redox couple[26] and a solid-state system comprised of the Y123 dye and the hole conductor spiro-OMeTAD[55]. Absorbing into the NIR region of the spectrum increases the photocurrent density from 20 mA cm$^{-2}$ to 30 mA cm$^{-2}$. **c**, Chemical structures of the best-performing ruthenium-based complex CYC-B11, together with donor–pi–acceptor dyes YD2-o-C8 and Y123. **d**, Chemical structures of the iodide redox couple, a cobalt redox mediator and the solid-state hole conductor spiro-OMeTAD.

**Table B1 | Power-conversion efficiency (PCE), short-circuit current density ($J_{SC}$), $V_{OC}$, fill factor, optimized titania thickness ($T$) and loss-in-potential for best-in class-DSCs.**

| Dye | Couple/conductor | Reference | PCE (%) | $J_{SC}$ (mA cm$^{-2}$) | $V_{OC}$ (mV) | Fill factor (%) | $T$ (μm) | Loss-in-potential (mV) |
|---|---|---|---|---|---|---|---|---|
| CYC-B11 | $I_3^-/I^-$ | 16 | 11.5 | 20.1 | 743 | 0.77 | 13 | 850 |
| YD2-o-C8 | $Co(bby)_3$ | 26 | 12.3 | 17.7 | 935 | 0.74 | 10 | 775 |
| Y123 | Spiro-OMeTAD | 55 | 7.1 | 9.5 | 986 | 0.77 | 2.5 | 890 |

improvements in dye design and the promise of removing expensive metals will result in not only increased power-conversion efficiencies but also greater potential to scale beyond 19 GW per year, which is the limit set by the availability of ruthenium[34].

Organic dyes generally have substantially higher molar extinction coefficients (50,000–200,000 M$^{-1}$ cm$^{-1}$) than ruthenium-based complexes, but typically have narrower spectral bandwidths ($\Delta\lambda \approx 100$–$250$ nm)[35–38]. Over the past few years, great strides have been made in understanding and designing new dyes for use in DSCs[8]. The best dyes contain both electron-rich (donor) and electron-poor (acceptor) sections connected through a conjugated (pi) bridge. The electron-poor section is functionalized with an acidic binding group that couples the molecule to the oxide surface. Photoexcitation causes a net electron transfer from the donor to acceptor sections such that the electron wavefunction couples to the titania conduction band states, while the hole wavefunction resides mostly away from the oxide surface where it is well-positioned to interact with the redox couple[8,39,40]. Alkyl chains are also often attached to the side of the dye to create a barrier between holes in the redox couple and electrons in the titania, thereby inhibiting recombination.

## The use of new redox couples to achieve higher voltages

Although scientists have discovered several alternative redox couples that are less corrosive than iodide and whose potentials are more suited to achieving high $V_{OC}$, solar cells containing such complexes typically have unacceptably high recombination rates and consequently poor performance (efficiencies of <5%). However, recent success using $Co^{2+}/Co^{3+}$ (refs 10,26,41,42), ferrocene $Fc/Fc^+$ (refs 43,44), copper I/II (refs 13,45) and all-organic[11,46,47] electrolytes have resulted in more promising power-conversion efficiencies.

In the past, $Co^{2+}/Co^{3+}$ electrolytes suffered from recombination rates that were at least an order of magnitude faster than iodide-based systems[10,42]. The $I^-/I_3^-$ couple is an elemental system, whereas $Co^{2+}$ and $Co^{3+}$ ions are surrounded by ligands that can be modified to modulate the redox potential (Fig. 2)[42]. Bulky groups on these ligands can function as insulating spacers, which slow down the recombination process between the electrolyte and the titania[42]. In 2010, Boschloo and co-workers demonstrated a significant improvement in the power-conversion efficiency of cobalt-based systems by adding bulky groups (such as insulating butoxyl chains) to an organic dye[41,48]. When the insulating ligands on the organic dye, which face away from the semiconductor, are used with the

bulky cobalt redox couple, recombination in the system is reduced by at least one order of magnitude without affecting the electron transfer rate. Grätzel and co-workers recently took this approach to the next level by applying the insulating ligand technique to a donor–pi–acceptor dye YD2-o-C8 (Fig. 2c), which has a broad absorption spectrum. In doing so, they achieved similarly low recombination rates and demonstrated DSCs with a laboratory-measured world record efficiency of 12.3% under 1 Sun illumination[26] (Table B1). The improved performance was linked to a 16% increase in $V_{OC}$ over cells containing an iodide-based redox couple, which demonstrates the importance of tuning the redox level to increase $V_{OC}$. The dye had an absorption onset at 725 nm and the cell had a total loss-in-potential of around 775 mV. In the short term, moving the dye absorption out to 830 nm could increase this efficiency to 13.6% without any further fundamental advances in technology. In recent work, an over-potential of only 390 mV was sufficient to regenerate the oxidized dye and achieve an external quantum efficiency of more than 80%[49]. Given a total loss-in-potential of 500 mV, and assuming a required over-potential of 100 mV on the electron-transfer side, it may be possible to increase the efficiency of the cobalt system to 19% by extending the absorption out to 920 nm (Fig. 3).

One of the shortcomings of cobalt-based complexes is that their bulky groups significantly decrease the speed at which the ions can diffuse through the electrolyte — up to an order of magnitude less than conventional iodide ions[50]. Grätzel and co-workers found that reducing the illumination intensity increased the power-conversion efficiency to 13.1%, as it is less important for the ions to diffuse to the electrode quickly when the carrier density is lower[26]. One could imagine obtaining this efficiency under 1 Sun illumination by using even thinner films to reduce the required diffusion distance. Later in this Review we will describe potential techniques for slowing recombination and attaining adequate light absorption in thin films.

Long-term stability studies have not yet been performed on cobalt complexes in dye-sensitized solar cells. It will be important to make sure that cobalt complexes do not undergo irreversible changes at the counter-electrode[42] while providing stabilities similar to (or better than) iodide-based electrolytes.

## Solid-state dye-sensitized solar cells

Solid-state DSCs (ss-DSCs), which use solid hole conductors instead of a liquid electrolyte, are also capable of delivering high voltages[51]. The hole conductor is typically made from either wide-bandgap small molecules (such as spiro-OMeTAD) or semiconducting polymers (such as PEDOT or P3HT). These DSCs are in principle more industrially compatible than standard DSCs because they do not contain a corrosive liquid electrolyte, which requires careful packaging. The highest values of $V_{OC}$ (>1 V) achieved so far have been demonstrated in devices that exploit a small-molecule hole conductor[52]. In ss-DSCs, hole transfer occurs directly from the oxidized dye to the HOMO level of the hole conductor, which then transports the charge to the (typically silver) counter-electrode[53,54]. Dye regeneration occurs over a period of tens to hundreds of picoseconds — several orders of magnitude faster than regeneration with the $I^-/I_3^-$ redox couple[53]. We believe that an over-potential of only 200 mV may be sufficient for hole regeneration, thus allowing for power-conversion efficiencies of more than 20%, as shown in Fig. 3 (again assuming a loss of 100 mV on the electron-transfer side). Although the first ss-DSCs made with solution-processable small molecules achieved power-conversion efficiencies of less than 1%, researchers have recently increased this value to 7.1%[51,55]. Significant recombination rates, together with the difficulty in achieving high levels of pore-filling in thicker films, means that ss-DSCs currently work best at thicknesses of only a few micrometres[56]. The greatest issues facing ss-DSCs are their incomplete light harvesting and lower internal quantum efficiency, which together result in current densities that are lower than liquid-based DSCs, as shown in Fig. 2 (Y123, a spiro-OMeTAD system)[55].

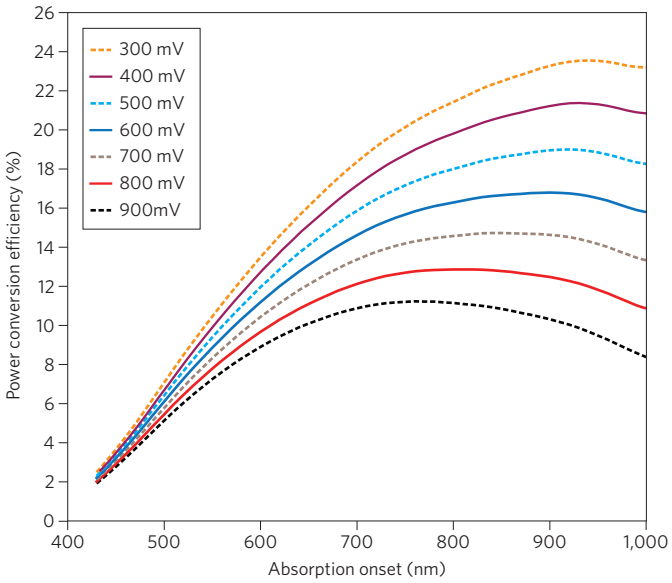


**Figure 3 | Maximum obtainable power-conversion efficiencies versus absorption onset for various loss-in-potentials.** The model assumes an external quantum efficiency of 90% with the rise from the onset of absorption occurring over a range of 50 nm and a constant fill factor of 0.75 (ref. 22).

There are many factors that affect the recombination between conduction-band electrons in the titania layer and holes in the hole conductor layer. Under solar operating conditions, the hole density in ss-DSCs is highest near the dye-sensitized interface (the point of generation) and charge screening is not as effective as it is in cells containing liquid electrolytes, which typically leads to recombination rates that are an order of magnitude larger than those in the best $I^-/I_3^-$ systems. Recombination in ss-DSCs can be significantly inhibited by interfacial engineering (discussed below) and having the correct mix of ionic additives in the hole transporter phase[54,57]. Chemical p-dopants are often added to the hole transporter to increase the conductivity, resulting in increased values of $V_{OC}$ and the fill factor[55].

Solid hole conductors are almost exclusively fabricated through solution-deposition techniques. However, pore-filling can never be complete through such procedures because space is left when the solvent evaporates[58,59]. The pore-filling fraction, which is defined as the fraction of porous volume taken by the hole conductor, can be as high as 60–80% with small-molecule hole conductors, and the pores are generally uniformly filled throughout the entire film thickness. Uniformly covering the dye/metal oxide surface is extremely important to ensure good charge separation and collection; as a rule of thumb, around 50% pore-filling is required in a mesoporous network to ensure monolayer surface coverage[59]. Improving the pore-filling fraction is an important strategy for reducing recombination and might be achieved by infiltrating hole conductors from the melt[60].

Light-harvesting in ss-DSCs has benefited tremendously from donor–pi–acceptor dyes, which provide significantly enhanced light absorption in 2-μm-thick films. Careful control over the p-dopant, in combination with the use of a strongly absorbing donor–pi–acceptor dye, has recently led to efficiencies of over 7% in ss-DSCs that exploit small-molecule hole conductors[55]. Another

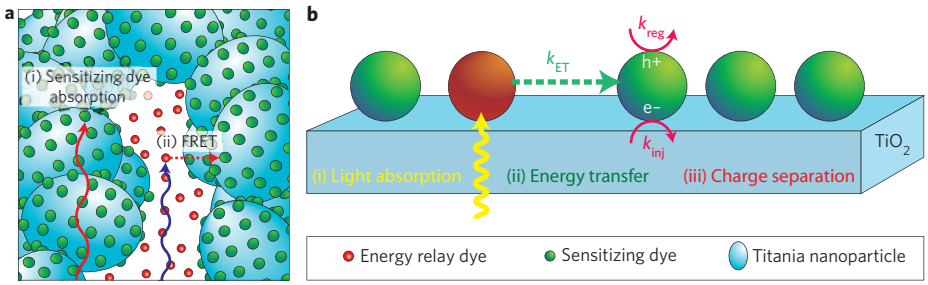


**Figure 4 | DSC containing ERDs. a**,**b**, ERDs mixed inside the liquid electrolyte (**a**) and co-sensitized to the titania surface (**b**). Typical absorption process for lower energy (red) photons in DSCs: light is absorbed by the sensitizing dye (i), after which an electron is transferred to the titania and a hole is transported to the back contact through the electrolyte. The ERD process is similar except that higher energy (blue) photons are first absorbed by the ERD and then undergo Förster resonant energy transfer (FRET; ii) at rate $k_{ET}$ to the sensitizing dye, which is responsible for charge separation (iii) involving electron injection (rate $k_{inj}$) and hole regeneration (rate $k_{reg}$).

way of improving light absorption in ss-DSCs is to use light-absorbing polymers as the hole conductor[61]. Polymer hole conductors, typically used in organic photovoltaic cells, have recently achieved power-conversion efficiencies of more than 5%[62]. Polymer hole conductors are also solution-processed, although the pore-filling fractions are much lower (<25%) than in small-molecule hole conductors. Despite this, however, the polymer can predominately wet the internal surface and carry holes efficiently out of devices of up to 7 μm in thickness[63].

Compared with their liquid-electrolyte counterparts, ss-DSCs have been significantly underdeveloped. Relatively few hole conductors have been studied for DSCs, and there are still no clearly defined rules for hole conductor design, doping and additive requirements, and dye modifications. Although optical models[64] have been created for ss-DSCs, understanding why the internal quantum efficiency (for example, charge generation/separation or charge collection) is lower for ss-DSCs than liquid-based DSCs will require much better knowledge of the physics of these devices. We believe significant improvements could be made by improving pore-filling and developing new hole conductors with deeper HOMO levels, additives to further reduce recombination and dyes that could result in a loss-in-potential of 300 mV.

## Engineering the interface to prevent recombination

In iodide-based DSCs, recombination is inherently slow and excessive electronic engineering of the interface is not entirely necessary. However, for both new electrolytes and solid-state hole conductor systems, fast recombination is a critical issue that must be reduced in order to realize maximum efficiency. It should be noted that a tenfold decrease in the recombination rate will result in a 50–60mV increase in $V_{OC}$ (ref. 5). The oxide can be surface-treated through either organic modification or inorganic shell growth. For organic modification, co-adsorption of surface modifiers alongside the dye molecules can be used to help block direct contact of the hole conductor or electrolyte with the titania, or to modify the energetics of the interface by introducing a dipolar field[65].

For inorganic modification, thin shells of 'insulating' oxides can be deposited on the titania layer prior to dye loading[66,67]. The insulating shell must be thin enough to allow electron transfer from the photoexcited dye, but also thick enough to inhibit the recombination reaction. Because the fundamental mechanism for both forwards electron transfer and recombination is the same, we expect the same inhibition in both rates. This technique therefore requires the initial electron transfer process to be faster than is strictly necessary, and to inhibit recombination only to the point at which a drop in photocurrent occurs because electron transfer to the titania is not occurring fast enough. In practice, there is usually a slight drop in photocurrent accompanied by an increase in $V_{OC}$. Researchers often overlook the fact that coating the surface of an oxide such as titania with an insulating shell usually results in a shift in the surface potential of the oxide. This usually causes an increase in $V_{OC}$ that can be mistakenly interpreted as being due to the inhibition of recombination.

Changing the ionic content in the hole conductor can be much more effective at slowing down recombination than introducing an inorganic shell (ref. 68). This is most likely caused by holes in the hole conductor electrostatically screening the electrons in the titania layer. Because the dielectric constant for titania is extremely large (~100$\varepsilon_0$), it is surprising that electrostatic screening is required once the electrons are transferred into the oxide. The fact that recombination is so sensitive to ionic additives suggests that the electrons undergoing recombination are in surface states and are not entirely screened by the bulk dielectric. Pacifying these surface states may therefore have a direct beneficial impact on charge recombination[69].

## Light trapping

In DSCs that do not contain the $I^-/I_3^-$ redox couple, it is a challenge to make the cell thick enough to absorb almost all of the light while also thin enough to ensure all the charge carriers are collected, as many of the carriers recombine before travelling more than a few micrometres. This problem can be avoided by scattering light in the cell to increase its path length or using plasmonic effects to intensify the absorption near nanopatterned metal.

The most commonly used light-trapping approach in cells containing liquid electrolytes is to deposit a film of titania particles measuring 200–400 nm in diameter on top of a layer of titania particles of normal size (20 nm, for example)[26,70]. The larger titania particles scatter light and thereby increase the photon path length in the cell[66]. In some cases, more well-ordered photonic crystals have been used to scatter light[71].

Alternative strategies are needed to trap light in ss-DSCs, whose thickness is limited to less than 3 μm. The use of plasmonic effects is particularly attractive for achieving this[72–75]. DSCs with plasmonic back-reflectors can be made by using nanoimprint lithography to press a hexagonal array of holes into a film of titania nanocrystals before the film is sintered. When the hole conductor infiltrates the film, it does not planarize the top surface. Consequently, when the silver electrode is deposited, it contains a patterned array of posts sticking into the solar cell that can scatter light very effectively and possibly couple it to plasmon–polariton modes[75]. Plasmonic back-reflectors have been shown to improve the performance of cells containing weakly absorbing ruthenium-based dyes by 20%, and cells containing strongly absorbing donor–pi–acceptor dyes by 5%[75]. Another plasmonic approach is to incorporate metal nanoparticles covered with an insulator or n-type oxide directly into the

solar cell[73,74]. Light excites the plasmon resonances of these particles and so significantly enhances the electric field (and therefore absorption) in the regions surrounding them.

Although light-trapping techniques are certainly helpful, the extent to which they can be used to solve absorption problems is limited because light-trapping also enhances parasitic absorption by the 'transparent' electrode and hole conductor.

## Co-sensitization and energy relay dyes

One of the greatest opportunities for improving the efficiency of all types of DSC is to reduce the energy gap of the dyes so that more light in the spectral range of 650–940 nm can be absorbed (Fig. 2a). However, finding one dye that absorbs strongly all the way from 350–940 nm is extremely difficult. Typically, the peak absorption coefficient and spectral width of a dye are inversely related to each other. The most promising strategy for harvesting the whole spectrum is to use a combination of visible- and NIR-absorbing dyes.

In the past, the co-sensitization of ruthenium metal complex dyes was considered to be problematic because their low molar extinction coefficient required full monolayer coverage on the titania of relatively thick films to absorb all the incident red photons. However, organic dyes have significantly higher molar extinction coefficients than ruthenium metal complex dyes and thus require smaller surface areas, making it possible to co-sensitize thinner DSC films without significantly reducing light-harvesting in any portion of the spectrum[76]. Today's record-efficiency DSC employs a co-sensitization strategy to boost absorption at a wavelength of 550 nm (ref. 26). Although co-sensitization for this device results in an overall increase in the power-conversion efficiency due to an increased short-circuit current density, $V_{OC}$ is reduced slightly because the co-sensitized dye used to absorb light at 550 nm is not as good at blocking recombination as the YD2-o-c8 dye with which the device is co-sensitized[26].

Only a few NIR dyes (that is, peak absorption at >700 nm) have so far demonstrated good charge injection efficiencies in DSCs, although no NIR dye has yet independently achieved a $V_{OC}$ greater than 460 mV in an electrolyte-based cell[77–79]. NIR-sensitizing dyes that do not require large over-potentials to regenerate and do not have high recombination rates will be required to push efficiencies towards 15%. The most significant challenge of co-sensitization using NIR dyes is maintaining a large $V_{OC}$, which requires that each dye adequately prevents recombination. The problem of $V_{OC}$ reduction is likely to be even more pronounced with NIR dyes because they have small bandgaps. The resulting energy and hole transfer from neighbouring visible sensitizing dyes[80] can increase recombination and lower $V_{OC}$ (ref. 81).

Energy relay dyes (ERDs) decouple the light-harvesting and charge-transfer processes, and therefore have a range of potential advantages over co-sensitization techniques. In DSCs, ERDs absorb sunlight and then transfer energy non-radiatively to sensitizing dyes, which are responsible for charge separation (Fig. 4)[82,83]. ERDs have been placed inside the electrolyte[82,84] and the semiconductor[85], co-sensitized[81,86–88] on the semiconductor surface, and tethered to sensitizing dyes[83]. The use of ERDs has several important advantages over co-sensitization. Because ERDs do not participate in the charge-transfer process, they do not require precise energy levels for charge transfer, which allows for a wide range of dyes to be implemented in DSC systems[82]. ERDs can be used to fill absorption gaps in the sensitizing dye for a liquid-based device, and also to increase the overall light-harvesting efficiency of solid-state systems[89]. ERDs do not need to attach to the semiconductor surface in order to contribute to light-harvesting, and thus their addition can both widen and strengthen the overall absorption spectrum for the same film thickness.

ERDs typically transfer energy via Förster resonant energy transfer, which involves dipole–dipole coupling between the ERD and the sensitizing dye[90]. The distance over which energy transfer can occur efficiently is determined primarily by the molar extinction coefficient of the sensitizing dye and the overlap between the emission spectrum of the ERD and the absorption spectrum of the sensitizing dye[91]. When designing ERDs, it is important to use dyes with relatively short photoluminescent lifetimes (<10 ns) because the rate of energy transfer depends on the rate of light emission and must therefore be faster than quenching by the electrolyte/hole conductor[82]. It is possible to use multiple ERDs to expand the overall spectral coverage[92].

Energy transfer may occur efficiently over fairly long distances (that is, >25 nm) for ERDs that have a strong emission overlap with the absorption spectrum of tightly packed organic dyes on the semiconductor surface[93]. This allows for high excitation transfer efficiencies of >90% for ERDs placed inside liquid-electrolyte systems[94] and >60% for ERDs placed in the hole conductor in ss-DSCs[95]. It has not yet been possible to dissolve enough ERDs into the electrolyte to absorb all of the light, although this should be possible to achieve by increasing the solubility and molar absorption coefficients of the ERDs[94]. It is still possible for systems with weaker dipole–dipole coupling to efficiently transfer energy over short distances, although this requires the ERDs to be within 1–3 nm of the sensitizing dye requiring co-sensitization[87] or tethering[83].

## The path to commercialization

The ultimate goal of any emerging solar cell technology is to achieve an installed cost-per-watt level that reaches grid parity versus conventional fossil fuel technologies and competes favourably against incumbent photovoltaic technologies. Silicon photovoltaic module costs have continued to reduce from US$4 $W^{-1}$ in 2008 to just US$1.25 $W^{-1}$ in 2011, with module efficiencies ranging from 15% to 20% and lifetimes guaranteed to 25 years. It is realistic to expect that silicon photovoltaic modules could continue to reduce in manufacturing costs to around US$0.70 $W^{-1}$, with module efficiencies rising to 18–22%. Great strides have also been made in the commercialization of thin-film technologies, where CdTe has achieved module efficiencies of 10–12.5% at costs of US$0.70 $W^{-1}$ and current roadmaps expect to achieve module efficiencies of 14% at costs of US$0.50 $W^{-1}$. Copper indium gallium selenide modules are now commercially available, with efficiencies of 12–15% and module costs expected to be less than US$0.50 $W^{-1}$.

How DSCs will compete in the future photovoltaic market depends not only on our ability to increase power-conversion efficiencies and develop ultralow-cost architectures that are stable over 20 years, but also on market factors such as the overall photovoltaic demand and the scarcity of rare elements. DCSs can be constructed from abundant non-toxic materials, which is a significant benefit over current thin-film technologies[1].

Commercializing 10%-efficient modules may require ultralow-cost architectures that reduce inherent costs by removing at least one glass substrate, thereby pushing costs down to US$20 $m^{-2}$. It is important to note there is an increased non-module 'balance-of-systems' cost associated with using less-efficient solar modules; for example, installing 10%-efficient modules costs US$0.30 $W^{-1}$ more than 15%-efficient modules[96]. 10%-efficient DSC modules will therefore probably need to be priced at US$0.20–0.30 $W^{-1}$ and thus manufactured at US$20–30 $m^{-2}$ to compete for utility-scale power generation. Substrates represent the largest module costs. At the gigawatt scale, glass covered with fluorine-doped tin oxide costs US$8–12 $m^{-2}$, whereas uncoated glass costs US$5 $m^{-2}$. The glass–glass laminate for DSCs would therefore cost at least US$13 $m^{-2}$, leaving only US$7–17 $m^{-2}$ for the remainder of manufacturing, which is possible but challenging.

Ultralow-cost DSCs could be built from cheap metal foils (such as stainless steel and aluminium) and plastic sheets to reduce glass costs. Although iodide is known to dissolve aluminium and stainless

steel, there is significant opportunity to create pinhole-free protective coatings on foils and develop electrolytes that are less corrosive than iodide. Additional stability issues emerge when using plastics sheets instead of glass, which have significantly higher water vapour transport rates and thus allow moisture to ingress into the DSC. Researchers have yet to produce a plastic sheet that is cheaper than glass while also having an adequate water vapour transport rate. Developing water-tolerant DSCs is an interesting pathway that is unique to this technology[97]. Furthermore, sputtered transparent conducting oxides on plastics are more expensive, less transparent and more resistive than when deposited on glass, which provides lower performance levels. Cheaper transparent conducting electrodes for DSCs must therefore be developed to match the efficiency of glass-based designs[98,99].

Increasing the module efficiencies of DSCs to more than 14% would relax the ultralow-cost constraints, thus providing substantial incentive to create laboratory-scale devices with efficiencies greater than 15%. The relatively slow increase in record values for DSCs over the past ten years has left the impression of a performance ceiling, which is partially justified given that conventional iodide- and ruthenium-based DSCs have a realistic maximum possible efficiency of little more than 13%[22]. The loss-in-potential can realistically be reduced to 500 mV by better matching the energy levels at the heterojunction, using more strongly absorbing dyes in thinner films and further inhibiting recombination losses, pushing efficiencies to 19% with a dye capable of absorbing out to 920 nm. Finally, although there have been a number of initial studies into the development of DSC modules, a thorough understanding of the overall lifetimes and degradation mechanisms of new DSC cell and module designs requires a great deal of further investigation[5,100].

## References


1. O'Regan, B. & Grätzel, M. A low-cost, high-efficiency solar cell based on dye-sensitized colloidal $TiO_2$ films. *Nature* **353,** 737–740 (1991).
2. Grätzel, M. Photoelectrochemical cells. *Nature* **414,** 338–344 (2001).
3. Hagfeldt, A. & Grätzel, M. Molecular photovoltaics. *Acc. Chem. Rec.* **33,** 269–277 (2000).
4. Ardo, S. & Meyer, G. J. Photodriven heterogeneous charge transfer with transition-metal compounds anchored to $TiO_2$ semiconductor surfaces. *Chem. Soc. Rev.* **38,** 115–164 (2009).
5. Hagfeldt, A., Boschloo, G., Sun, L., Kloo, L. & Pettersson, H. Dye-sensitized solar cells. *Chem. Rev.* **110,** 6595–6663 (2010).
6. Green, M. A., Emery, K., Hishikawa, Y., Warta, W. & Dunlop, E. D. Solar cell efficiency tables (version 38). *Prog. Photovolt. Res. Appl.* **19,** 565–572 (2011).
7. Robertson, N. Optimizing dyes for dye-sensitized solar cells. *Angew. Chem. Int. Ed.* **45,** 2338–2345 (2006).
8. Mishra, A., Fischer, M. K. R. & Bäuerle, P. Metal-free organic dyes for dye-sensitized solar cells: From structure–property relationships to design rules. *Angew. Chem. Int. Ed.* **48,** 2474–2499 (2009).
9. Oskam, G., Bergeron, B. V., Meyer, G. J. & Searson, P. C. Pseudohalogens for dye-sensitized $TiO_2$ photoelectrochemical cells. *J. Phys. Chem. B* **105,** 6867–6873 (2001).
10. Nusbaumer, H., Moser, J.-E., Zakeeruddin, S. M., Nazeeruddin, M. K. & Grätzel, M. $Co^{II}(dbbip)_2^{2+}$ complex rivals tri-iodide/iodide redox mediator in dye-sensitized photovoltaic cells. *J. Phys. Chem. B* **105,** 10461–10464 (2001).
11. Zhang, Z., Chen, P., Murakami, T. N., Zakeeruddin, S. M. & Grätzel, M. The 2,2,6,6-tetramethyl-1-piperidinyloxy radical: An efficient, iodine-free redox mediator for dye-sensitized solar cells. *Adv. Funct. Mater.* **18,** 341–346 (2008).
12. Wang, P., Zakeeruddin, S. M., Moser, J.-E., Humphry-Baker, R. & Grätzel, M. A solvent-free, $SeCN^-/(SeCN)_3^-$ based ionic liquid electrolyte for high-efficiency dye-sensitized nanocrystalline solar cells. *J. Am. Chem. Soc.* **126,** 7164–7165 (2004).
13. Hattori, S., Wada, Y., Yanagida, S. & Fukuzumi, S. Blue copper model complexes with distorted tetragonal geometry acting as effective electron-transfer mediators in dye-sensitized solar cells. *Jpn. J. Appl. Phys.* **127,** 9648–9654 (2005).
14. Nazeeruddin, M. K. *et al.* Combined experimental and DFT–TDDFT computational study of photoelectrochemical cell ruthenium sensitizers. *J. Am. Chem. Soc.* **127,** 16835–16847 (2005).
15. Gao, F. *et al.* Enhance the optical absorptivity of nanocrystalline $TiO_2$ film with high molar extinction coefficient ruthenium sensitizers for high performance dye-sensitized solar cells. *J. Am. Chem. Soc.* **130,** 10720–10728 (2008).
16. Chen, C.-Y. *et al.* Highly efficient light-harvesting ruthenium sensitizer for thin-film dye-sensitized solar cells. *ACS Nano* **3,** 3103–3109 (2009).
17. Chiba, Y. *et al.* Dye-sensitized solar cells with conversion efficiency of 11.1%. *Jpn. J. Appl. Phys.* **45,** 638–640 (2006).
18. Huang, S., Schlichthorl, G., Nozik, A., Grätzel, M. & Frank, A. Charge recombination in dye-sensitized nanocrystalline $TiO_2$ solar cells. *J. Phys. Chem. B* **101,** 2576–2582 (1997).
19. Boschloo, G. & Hagfeldt, A. Characteristics of the iodide/triiodide redox mediator in dye-sensitized solar cells. *Acc. Chem. Rec.* **42,** 1819–1826 (2009).
20. Bisquert, J., Fabregat-Santiago, F., Mora-Seró, I. N., Garcia-Belmonte, G. & Giménez, S. Electron lifetime in dye-sensitized solar cells: Theory and interpretation of measurements. *J. Phys. Chem. C* **113,** 17278–17290 (2009).
21. Shockley, W. & Queisser, H. J. Detailed balance limit of efficiency of p–n junction solar cells. *J. Appl. Phys.* **32,** 510–519 (1961).
22. Snaith, H. J. Estimating the maximum attainable efficiency in dye-sensitized solar cells. *Adv. Funct. Mater.* **20,** 13–19 (2010).
23. Koops, S. E., O'Regan, B. C., Barnes, P. R. F. & Durrant, J. R. Parameters influencing the efficiency of electron injection in dye-sensitized solar cells. *J. Am. Chem. Soc.* **131,** 4808–4818 (2009).
24. Hamann, T. W., Jensen, R. A., Martinson, A. B. F., Ryswyk, H. V. & Hupp, J. T. Advancing beyond current generation dye-sensitized solar cells. *Energ. Environ. Sci.* **1,** 66–78 (2008).
25. Peter, L. M. The Grätzel cell: Where next? *J. Phys. Chem. Lett.* **2,** 1861–1867 (2011).
26. Yella, A. *et al.* Porphyrin-sensitized solar cells with cobalt(II/III)-based redox electrolyte exceed 12 percent efficiency. *Science* **334,** 629–634 (2011).
27. Peter, L. M. Dye-sensitized nanocrystalline solar cells. *Phys. Chem. Chem. Phys.* **9,** 2630–2642 (2007).
28. Snaith, H. J. & Schmidt-Mende, L. Advances in liquid-electrolyte and solid-state dye-sensitized solar cells. *Adv. Mater.* **19,** 3187–3200 (2007).
29. Grätzel, M. Conversion of sunlight to electric power by nanocrystalline dye-sensitized solar cells. *J. Photochem. Photobiol. A* **164,** 3–14 (2004).
30. Grätzel, M. Solar energy conversion by dye-sensitized photovoltaic cells. *Inorg. Chem.* **44,** 6841–6851 (2005).
31. Listorti, A., O'Regan, B. & Durrant, J. R. Electron transfer dynamics in dye-sensitized solar cells. *Chem. Mater.* **23,** 3381–3399 (2011).
32. Nazeeruddin, M. K. *et al.* Engineering of efficient panchromatic sensitizers for nanocrystalline $TiO_2$-based solar cells. *J. Am. Chem. Soc.***123,** 1613–1624 (2001).
33. Nazeeruddin, M. K. *et al.* Conversion of light to electricity by *cis*-$X_2$bis(2,2'-bipyridyl-4,4'-dicarboxylate)ruthenium(II) charge-transfer sensitizers ($X$ = $Cl^-$, $Br^-$, $I^-$, $CN^-$, and $SCN^-$) on nanocrystalline titanium dioxide electrodes. *J. Am. Chem. Soc.* **115,** 6382–6390 (1993).
34. http://minerals.usgs.gov/minerals/pubs/commodity/platinum/myb1-2010-plati.pdf
35. Horiuchi, T., Miura, H., Sumioka, K. & Uchida, S. High efficiency of dye-sensitized solar cells based on metal-free indoline dyes. *J. Am. Chem. Soc.***126,** 12218–12219 (2004).
36. Yum, J.-H. *et al.* Efficient far red sensitization of nanocrystalline $TiO_2$ films by an unsymmetrical squaraine dye. *J. Am. Chem. Soc.* **129,** 10320–10321 (2007).
37. Campbell, W. M. *et al.* Highly efficient porphyrin sensitizers for dye-sensitized solar cells. *J. Phys. Chem. C* **111,** 11760–11762 (2007).
38. He, J. *et al.* Modified phthalocyanines for efficient near-IR sensitization of nanostructured $TiO_2$ electrode. *J. Am. Chem. Soc.* **124,** 4922–4932 (2002).
39. Bessho, T., Zakeeruddin, S. M., Yeh, C.-Y., Diau, E. W.-G. & Grätzel, M. Highly efficient mesoscopic dye-sensitized solar cells based on donor–acceptor-substituted porphyrins. *Angew. Chem. Int. Ed.* **49,** 6646–6649 (2010).
40. Lee, C.-W. *et al.* Novel zinc porphyrin sensitizers for dye-sensitized solar cells: Synthesis and spectral, electrochemical, and photovoltaic properties. *Chem. Euro. J.* **15,** 1403–1412 (2009).
41. Feldt, S. M. *et al.* Design of organic dyes and cobalt polypyridine redox mediators for high-efficiency dye-sensitized solar cells. *J. Am. Chem. Soc.* **132,** 16714–16724 (2010).
42. Sapp, S. A., Elliott, C. M., Contado, C., Caramori, S. & Bignozzi, C. A. Substituted polypyridine complexes of cobalt(II/III) as efficient electron-transfer mediators in dye-sensitized solar cells. *J. Am. Chem. Soc.* **124,** 11215–11222 (2002).
43. Gregg, B. A., Pichot, F., Ferrere, S. & Fields, C. L. Interfaical recombination processes in dye-sensitized solar cells and methods to passivate the interfaces. *J. Phys. Chem. B* **105,** 1422–1429 (2001).

44. Daeneke, T. *et al.* High-efficiency dye-sensitized solar cells with ferrocene-based electrolytes. *Nature Chem.* **3,** 211–215 (2011).
45. Bai, Y. *et al.* High-efficiency organic dye-sensitized mesoscopic solar cells with a copper redox shuttle. *Chem. Commun.* **47,** 4376–4378 (2011).
46. Wang, M. *et al.* An organic redox electrolyte to rival triiodide/iodide in dye-sensitized solar cells. *Nature Chem.* **2,** 385–389 (2010).
47. Tian, H., Yu, Z., Hagfeldt, A., Kloo, L. & Sun, L. Organic redox couples and organic counter electrode for efficient organic dye-sensitized solar cells. *J. Am. Chem. Soc.* **133,** 9413–9422 (2011).
48. Klahr, B. M. & Hamann, T. W. Performance enhancement and limitations of cobalt bipyridyl redox shuttles in dye-sensitized solar cells. *J. Phys. Chem. C* **113,** 14040–14045 (2009).
49. Feldt, S. M., Wang, G., Boschloo, G. & Hagfeldt, A. Effects of driving forces for recombination and regeneration on the photovoltaic performance of dye-sensitized solar cells using cobalt polypyridine redox couples. *J. Phys. Chem. C* **115,** 21500–21507 (2011).
50. Nelson, J. J., Amick, T. J. & Elliott, C. M. Mass transport of polypyridyl cobalt complexes in dye-sensitized solar cells with mesoporous $TiO_2$ photoanodes. *J. Phys. Chem. C* **112,** 18255–18263 (2008).
51. Bach, U. *et al.* Solid-state dye-sensitized mesoporous $TiO_2$ solar cells with high photon-to-electron conversion efficiencies. *Nature* **395,** 583–585 (1998).
52. Chen, P. *et al.* High open-circuit voltage solid-state dye-sensitized solar cells with organic dye. *Nano Lett.* **9,** 2487–2492 (2009).
53. Bach, U. *et al.* Charge separation in solid-state dye-sensitized heterojunction solar cells. *J. Am. Chem. Soc.* **121,** 7445–7446 (1999).
54. Snaith, H. J. *et al.* Efficiency enhancements in solid-state hybrid solar cells via reduced charge recombination and increased light capture. *Nano Lett.* **7,** 3372–3376 (2007).
55. Burschka, J. *et al.* Tris(2-(1H-pyrazol-1-yl)pyridine)cobalt(III) as p-type dopant for organic semiconductors and its application in highly efficient solid-state dye-sensitized solar cells. *J. Am. Chem. Soc.* **133,** 18042–18045 (2011).
56. Schmidt-Mende, L., Kroeze, J. E., Durrant, J. R., Nazeeruddin, M. K. & Grätzel, M. Effect of hydrocarbon chain length of amphiphilic ruthenium dyes on solid-state dye-sensitized photovoltaics. *Nano Lett.* **5,** 1315–1320 (2005).
57. Krüger, J., Plass, R., Grätzel, M., Cameron, P. J. & Peter, L. M. Charge transport and back reaction in solid-state dye-sensitized solar cells: A study using intensity-modulated photovoltage and photocurrent spectroscopy. *J. Phys. Chem. B* **107,** 7536–7539 (2003).
58. Snaith, H. J. *et al.* Charge collection and pore filling in solid-state dye-sensitized solar cells *Nanotechnology* **19,** 424003 (2008).
59. Ding, I. K. *et al.* Pore-filling of spiro-OMeTAD in solid-state dye-sensitized solar cells: Quantification, mechanism, and consequences for device performance. *Adv. Func. Mater.* **19,** 2431–2436 (2009).
60. Melas-Kyriazi, J. *et al.* The effect of hole transport material pore filling on photovoltaic performance in solid-state dye-sensitized solar cells. *Adv. Eng. Mater.* **1,** 407–414 (2011).
61. Zhu, R., Jiang, C.-Y., Liu, B. & Ramakrishna, S. Highly efficient nanoporous $TiO_2$-polythiophene hybrid solar cells based on interfacial modification using a metal-free organic dye. *Adv. Mater.* **21,** 994–1000 (2009).
62. Chang, J. A. *et al.* High-performance nanostructured inorganic–organic heterojunction solar cells. *Nano Lett.* **10,** 2609–2612 (2010).
63. Abrusci, A. *et al.* Facile infiltration of semiconducting polymer into mesoporous electrodes for hybrid solar cells. *Energ. Environ. Sci.* **4,** 3051–3058 (2011).
64. Moulé, A. J. *et al.* Optical description of solid-state dye-sensitized solar cells. I. Measurement of layer optical properties. *J. Appl. Phys.* **106,** 073111 (2009).
65. Wang, M. *et al.* Surface design in solid-state dye sensitized solar cells: Effects of zwitterionic co-adsorbents on photovoltaic performance. *Adv. Func. Mater.* **19,** 2163–2172 (2009).
66. Palomares, E., Clifford, J. N., Haque, S. A., Lutz, T. & Durrant, J. R. Control of charge recombination dynamics in dye sensitized solar cells by the use of conformally deposited metal oxide blocking layers. *J. Am. Chem. Soc.* **125,** 475–482 (2003).
67. Palomares, E., Clifford, J. N., Haque, S. A., Lutz, T. & Durrant, J. R. Slow charge recombination in dye-sensitised solar cells (DSSC) using $Al_2O_3$ coated nanoporous $TiO_2$ films. *Chem. Commun.* 1464–1465 (2002).
68. Kruger, J. *et al.* High efficiency solid-state photovoltaic device due to inhibition of interface charge recombination. *Appl. Phys. Lett.* **79,** 2085–2087 (2001).
69. Fabregat-Santiago, F. *et al.* The origin of slow electron recombination processes in dye-sensitized solar cells with alumina barrier coatings. *J. Appl. Phys.* **96,** 6903–6907 (2004).
70. Ito, S. *et al.* Fabrication of thin film dye sensitized solar cells with solar to electric power conversion efficiency over 10%. *Thin Solid Films* **516,** 4613–4619 (2008).
71. Nishimura, S. *et al.* Standing wave enhancement of red absorbance and photocurrent in dye-sensitized titanium dioxide photoelectrodes coupled to photonic crystals. *J. Am. Chem. Soc.* **125,** 6306–6310 (2003).
72. Hagglund, C., Zach, M. & Kasemo, B. Enhanced charge carrier generation in dye sensitized solar cells by nanoparticle plasmons. *Appl. Phys. Lett.* **92,** 013113 (2008).
73. Standridge, S. D., Schatz, G. C. & Hupp, J. T. Distance dependence of plasmon-enhanced photocurrent in dye-sensitized solar cells. *J. Am. Chem. Soc.* **131,** 8407–8409 (2009).
74. Brown, M. D. *et al.* Plasmonic dye-sensitized solar cells using core–shell metal–insulator nanoparticles. *Nano Lett.* **11,** 438–445 (2010).
75. Ding, I. K. *et al.* Plasmonic dye-sensitized solar cells. *Adv. Energ. Mater.* **1,** 52–57 (2011).
76. Cid, J.-J. *et al.* Molecular cosensitization for efficient panchromatic dye-sensitized solar cells. *Angew. Chem. Int. Ed.* **119,** 8510–8514 (2007).
77. Ono, T., Yamaguchi, T. & Arakawa, H. Study on dye-sensitized solar cell using novel infrared dye. *Sol. Energ. Mater. Sol. C.* **93,** 831–835 (2009).
78. Macor, L. *et al.* Near-IR sensitization of wide band gap oxide semiconductor by axially anchored Si-naphthalocyanines. *Energ. Environ. Sci.* **2,** 529–534 (2009).
79. Maeda, T. *et al.* Near-infrared absorbing squarylium dyes with linearly extended π-conjugated structure for dye-sensitized solar cell applications. *Org. Lett.* **13,** 5994–5997 (2011).
80. Sayama, K. *et al.* Efficient sensitization of nanocrystalline $TiO_2$ films with cyanine and merocyanine organic dyes. *Sol. Energ. Mater. Sol. C.* **80,** 47–71 (2003).
81. Hardin, B. E. *et al.* Energy and hole transfer between dyes attached to titania in cosensitized dye-sensitized solar cells. *J. Am. Chem. Soc.* **133,** 10662–10667 (2011).
82. Hardin, B. E. *et al.* Increased light harvesting in dye-sensitized solar cells with energy relay dyes. *Nature Photon.* **3,** 406–411 (2009).
83. Siegers, C. *et al.* A dyadic sensitizer for dye solar cells with high energy-transfer efficiency in the device. *Chem. Phys. Chem.* **8,** 1548–1556 (2007).
84. Shankar, K., Feng, X. & Grimes, C. A. Enhanced harvesting of red photons in nanowire solar cells: Evidence of resonance energy transfer. *ACS Nano* **3,** 788–794 (2009).
85. Buhbut, S. *et al.* Built-in quantum dot antennas in dye-sensitized solar cells. *ACS Nano* **4,** 1293–1298 (2010).
86. Siegers, C. *et al.* Overcoming kinetic limitations of electron injection in the dye solar cell via coadsorption and FRET. *Chem. Phys. Chem.* **9,** 793–798 (2008).
87. Griffith, M. J. *et al.* Remarkable synergistic effects in a mixed porphyrin dye-sensitized $TiO_2$ film. *Appl. Phys. Lett.* **98,** 163502 (2011).
88. Brown, M. D. *et al.* Surface energy relay between cosensitized molecules in solid-state dye-sensitized solar cells. *J. Phys. Chem. C* **115,** 23204–23208 (2011).
89. Yum, J. H. *et al.* Panchromatic response in solid-state dye-sensitized solar cells containing phosphorescent energy relay dyes. *Angew. Chem. Int. Ed.* **48,** 9277–9280 (2009).
90. Förster, T. Transfer mechanisms of electronic excitation. *Discuss. Faraday Soc.* **27,** 7 (1959).
91. Lakowicz, J. R. *Principles of Fluorescence Spectroscopy* Ch. 13–15 (Plenum, 1999).
92. Yum, J.-H. *et al.* Incorporating multiple energy relay dyes in liquid dye-sensitized solar cells. *Chem. Phys. Chem.* **12,** 657–661 (2011).
93. Hoke, E. T., Hardin, B. E. & McGehee, M. D. Modeling the efficiency of Förster resonant energy transfer from energy relay dyes in dye-sensitized solar cells. *Opt. Express* **18,** 3893–3904 (2010).
94. Hardin, B. E. *et al.* High excitation transfer efficiency from energy relay dyes in dye-sensitized solar cells. *Nano Lett.* **10,** 3077–3083 (2010).
95. Mor, G. K. *et al.* High-efficiency Förster resonance energy transfer in solid-state dye sensitized solar cells. *Nano Lett.* **10,** 2387–2394 (2010).
96. http://www1.eere.energy.gov/solar/sunshot/pdfs/dpw_lushetsky.pdf.
97. Law, C. *et al.* Water-based electrolytes for dye-sensitized solar cells. *Adv. Mater.* **22,** 4505–4509 (2010).
98. Gaynor, W., Burkhard, G. F., McGehee, M. D. & Peumans, P. Smooth nanowire/polymer composite transparent electrodes. *Adv. Mater.* **23,** 2905–2910 (2011).
99. Hardin, B. E. *et al.* Laminating solution-processed silver nanowire mesh electrodes onto solid-state dye-sensitized solar cells. *Org. Electron.* **12,** 875–879 (2011).
100. Asghar, M. I. *et al.* Review of stability for advanced dye solar cells. *Energ. Environ. Sci.* **3,** 418–426 (2010).